



ORIGINAL RESEARCH ARTICLE

Inverse Problem in the Stochastic Approach to Modeling of Phase Transformations in Steels during Cooling after Hot Forming

Danuta Szeliga , Jakub Foryś, Natalia Jażdżewska , Jan Kusiak , Rafał Nadolski , Piotr Oprocha , Maciej Pietrzyk , Paweł Potorski , and Paweł Przybyłowicz

Submitted: 18 February 2024 / Revised: 23 October 2024 / Accepted: 29 October 2024 / Published online: 29 November 2024

The motivation for this research was the need for a reliable prediction of the distribution of microstructural parameters in steels during thermomechanical processing. The stochastic model describing the evolution of dislocation populations and grain size, which considers the random phenomena occurring during the hot forming of metallic alloys, was extended by including phase transformations during cooling. Accounting for a stochastic character of the nucleation of the new phase is the main feature of the model. Steel was selected as an example of the metallic alloy and equations describing the nucleation probability were proposed for ferrite, pearlite and bainite. The accuracy and reliability of the model depends on the correctness of the determination of the coefficients corresponding to the specific material. In the present paper these coefficients were identified using the inverse analysis for the experimental data. Experiments composed constant cooling rate tests for cooling rates in the range 0.1–20 °C/s. The inverse approach to a nonlinear model is ill-conditioned and must be transferred into an optimization problem, which requires formulating the appropriate objective function. Since the model is stochastic, it was a crucial, yet demanding task. The objective function based on a metric of the distance between measured and calculated histograms was proposed to achieve this goal. The original stochastic approach to identifying the phase transformation model for steels was tested, and an appropriate optimization strategy was proposed.

Keywords heterogeneous microstructures, identification, multiphase steels, nucleation, optimization, phase transformations, stochastic model

1. Introduction

Numerical models, which can predict the evolution of various microstructural parameters in metallic materials, have been intensively investigated during the last few decades. Numerous equations describing the evolution of the microstructure during hot forming and during phase transformations have been developed. A review of the phenomenological microstructure evolution models, commonly used in the second half of the twentieth century, is presented in (Ref 1). Recently, mean-field and full-field material models have been distinguished in the literature (Ref 2, 3). Thorough review of these two groups of models is presented in the PhD thesis (Ref 4). In the mean-field models, the microstructure is implicitly represented by equations describing the dislocation density (uniform per grain), the

average grain size, the kinetics of phase transformations, etc. The full-field models are based on an explicit representation of the microstructure using either the representative volume element (RVE) (Ref 5) or the digital materials representation (DMR) concept (Ref 6). From one side, the full-field models have extensive predictive capabilities and are much more comprehensive. On the other side, they involve large computing costs.

Deterministic calculations, which are based exclusively on either mean-field or full-field models, have some limitations. Observations of different metallic materials show that deterministic models are often too idealized and do not adequately reflect the complexity of the heterogeneous microstructure. For example, the prediction of grain structure during hot forming may be difficult because the size of the recrystallized and non-recrystallized grains may vary significantly. To include these aspects in modeling, it is necessary to consider distributions (histograms) of the microstructural parameters instead of their average values. Moreover, such microstructural phenomena as recrystallization and nucleation during phase transformation are stochastic in their nature and they appear with certain probability. Thus, stochastic microstructure evolution models are needed to describe these phenomena.

Accounting for stochasticity of the microstructure evolution is common in the scientific literature (Ref 7). Many applications are dedicated to solidification (Ref 8) and to fluid flow computations (Ref 9). The primary attempt to introduce stochasticity in plastic deformation was proposed in (Ref 10), where the stochastic contours of the propagating dislocation fronts are modeled. Several publications describing stationary

Danuta Szeliga, Jakub Foryś, Jan Kusiak, Rafał Nadolski, and Maciej Pietrzyk, Faculty of Metals Engineering and Industrial Computer Science, AGH University of Krakow, Al. Mickiewicza 30, 30-059 Kraków, Poland; Natalia Jażdżewska, Piotr Oprocha, Paweł Potorski, and Paweł Przybyłowicz, Faculty of Applied Mathematics, AGH University of Krakow, Al. Mickiewicza 30, 30-059 Kraków, Poland. Contact e-mail: madolsk@agh.edu.pl.

and non-stationary state stochastic models of the evolution of dislocations are discussed in earlier paper (Ref 11). The model, which considers the stochastic character of recrystallization occurring during hot forming and describes the evolution of the dislocations and the grain size, was formulated in Ref 12. The coefficients in this model were identified on the basis of experimental data, and the validated version of the model with examples of applications is presented in (Ref 13). However, since cooling after hot forming decides about the properties of final products, the hot forming model was extended by including phase transformations. The histograms of the dislocation density and the grain size, calculated by the stochastic hot deformation model, were used as an input for the simulation of phase transformations. Accounting for the stochastic character of the nucleation of the new phase and solution of the differential evolution equation for stochastic variables was the main objective of the present work. Stochasticity of the solution is caused by both random input and random character of the nucleation. Phase transformation model preceded by developed earlier hot deformation model will be capable of simulating the whole manufacturing cycle composed of hot forming and controlled cooling. In consequence, fast calculations (mean-field model) of evolution of heterogeneous microstructure during the whole manufacturing cycle can be performed and uncertainty of the final microstructure can be evaluated.

2. Motivation and Objectives

Modern construction materials should combine high strength with a good workability and have a high strength-to-density ratio. Multiphase steels with heterogeneous microstructures (the advanced high strength steels—AHSS) meet these requirements and they have been of interest of researchers for the last few decades (Ref 14, 15). Microstructure of these steels is composed of ferrite matrix with hard islands of bainite, martensite and sometimes retained austenite. Dual phase (DP) and complex phase (CP) are leading examples of the AHSSs, which are commonly used in the automotive industry (Ref 16). Both these steels have good strength and good global formability, represented by elongation in the tensile tests. The microstructure and mechanical properties have been extensively studied for DP steels (Ref 17), and it was observed that combination of the soft ferrite matrix with hard islands of martensite results in the high strength and total elongation. On the other hand, it involves affects local formability due to sharp gradients of properties at the interfaces. On the contrary, CP steels with a heterogeneous mixture of bainite, martensite and ferrite have smoother gradients of properties and better local formability (Ref 15, 18), which make them suitable for stretch-forming processes (Ref 19).

Beyond predictions of the microstructure heterogeneities, a problem of the uncertainty of these predictions is also essential and it is a significant challenge for modeling (Ref 20). Knowing the possible spread of the predicted microstructural parameters is important for technologists.

Two hypotheses were formulated on the basis of the discussion above: (i) The properties of the multiphase steels can be still improved by tailoring microstructural gradients (Ref 21). These gradients are due to the distributions of the grain size and the dislocation density, as well as to crystallographic texture and segregation of elements (Ref 15); (ii) a reliable

process design for manufacturing multiphase steels requires full knowledge about possible spread of the predicted output parameters, such as phase composition or ferrite grain size. The uncertainty of the predictions is caused mainly by a lack of repeatability of the boundary conditions caused by uncertainty of the process conditions and the stochastic character of the material behavior. Advanced numerical models, which are based on the multiphysics and multiscale approach, and which account for a stochastic character of the microstructure evolution, are needed to prove the two hypotheses and to support design of processing of the multiphase steels. Although the reasons for the heterogeneity and uncertainty of the predictions are different, the stochastic model proposed in the present work can be used to investigate both these aspects.

Review of the literature shows that majority of the publications treating about stochastic approach to the inverse problem is dedicated to the uncertainty of the inverse solution. Authors of these publications consider deterministic material model and investigate the uncertainty of the identification of these models. For example, in (Ref 22) a statistical information about an observed state variable in a system is used to estimate probabilistically unknown parameters through the solution of a stochastic optimization problem. The present paper is dedicated to the development, identification and verification of the stochastic phase transformations model, which calculates distributions (histograms) of microstructural features. The main focus is on the formulation of the inverse problem applied to the identification of this stochastic model, which justifies the scientific importance of the research. The inverse approach preceded the sensitivity analysis and solution of the inverse problem dedicated to the identification of the coefficients in the model. Application of the inverse approach to the identification of the stochastic model stochastic equations describing the nucleation of ferrite, pearlite and bainite were proposed in (Ref 23) and primary evaluation of these equations was performed. The emphasis was put on the sensitivity analysis (SA) of the model and evaluation of the importance of various coefficients. Local SA was applied and the sensitivity factor was calculated using the finite difference method. It was observed in (Ref 23) that due to the mutual interrelation between transformations, the non-physical influence of the coefficients was observed when the increment of the coefficient in the finite difference method was too large. It may cause problems during optimization in the inverse solution when the search space is large. Thus, in the present work, the SA was extended by evaluation of the influence of the coefficients increments on the sensitivity factors.

Formulation of the inverse problem dedicated to the identification of the stochastic model was the main contribution of the present work. A metric of the distance between measured and calculated histograms of microstructural parameters was used as the objective function for the inverse analysis, which is a novel approach. Various optimization procedures for this objective function were investigated, and the best optimization strategy was proposed.

3. Stochastic Model of Phase Transformations

The developed model introduces stochastic aspect in modeling microstructure evolution. It follows the idea described in earlier publication (Ref 12) for recrystallization

Table 1 Equations describing equilibrium carbon concentrations [23]

Carbon concentration at the γ/α interface line GS	Carbon concentration at the $\gamma/\text{cementite}$ interface—line ES
$c_{\gamma\alpha} = c_{\gamma\alpha 0} + c_{\gamma\alpha 1}T(t)$ (1)	$c_{\gamma\beta} = c_{\gamma\beta 0} + c_{\gamma\beta 1}T(t)$ (2)

during hot deformation. The model simulates phase transformations occurring in steels during controlled cooling, which takes place after hot deformation processes. The following structural components in steels are considered: austenite, ferrite, pearlite, bainite and martensite. It is assumed that at high temperature the microstructure is fully austenitic. At the end of the cooling process, the four remaining phases occupy the whole volume of the material. The retained austenite, which can appear under certain specific cooling conditions, is not considered.

The model accounts for the stochastic character of the input data (austenite grain size and dislocation density after hot deformation are in the form of histograms) and for the random character of the nucleation of the new phase. The growth of the phases is described by a deterministic equation. The output of the model consists of transformation temperatures and phase volume fractions presented in the form of either histograms or average values of these parameters calculated based on the histograms. In the paper, the former will be referred to as the stochastic output and the latter as the average output.

3.1 State of the Equilibrium

The phase transformation model describes the kinetics of the transient state between the two equilibrium states, which are described by the thermodynamics. The equilibrium for steels is described by the phase equilibrium diagram Fe-Fe₃C. Approximation of the lines GS and ES in this diagram gives the equations in Table 1, where T is the temperature in °C, t is the time $c_{\gamma\alpha 0}$, $c_{\gamma\alpha 1}$, $c_{\gamma\beta 0}$ and $c_{\gamma\beta 1}$ —coefficients, which were determined using ThermoCalc software by researchers from the Upper-Silesian Institute of Technology (see joint publication (Ref 24)). The following values of these were obtained: $c_{\gamma\alpha 0} = 4.677$, $c_{\gamma\alpha 1} = -0.00555$, $c_{\gamma\beta 0} = -1.0387$ and $c_{\gamma\beta 1} = 0.0024$.

The current average carbon content in the austenite c_γ increases with an increase of the ferrite volume fraction:

$$c_\gamma = \frac{c_0 - F_f c_\alpha}{1 - F_f} \quad (\text{Eq 3})$$

where c_0 —carbon content in steel, F_f —ferrite volume fraction with respect to the whole volume, c_α —carbon content in ferrite.

Other parameters in the model are: A_{e3} , A_{e1} —theoretical temperatures of the beginning and the end of the ferritic transformation, c_{eut} —equilibrium carbon concentration at the eutectic temperature, calculated as a cross point of lines (Eq 1) and (Eq 2):

$$c_{\text{eut}} = c_{\gamma\alpha 0} + c_{\gamma\alpha 1} \frac{c_{\gamma\alpha 0} - c_{\gamma\beta 0}}{c_{\gamma\alpha 1} - c_{\gamma\beta 1}} \quad (\text{Eq 4})$$

The equilibrium volume fraction of ferrite at the temperature A_{e1} is calculated from the following equation:

$$F_{\text{eut}} = \frac{c_{\text{eut}} - c_0}{c_{\text{eut}} - c_\alpha} \quad (\text{Eq 5})$$

Equilibrium parameters determined by Eqs 1, 2, and 3-5 were used as boundary conditions for the model, which describes the kinetics of phase transformations.

3.2 Nucleation of a New Phase

The nucleation is an initial step of each transformation. The nucleation model has to describe how nuclei appear in time and their nuclei locations. In the classical JMAK (Johnson-Mehl-Avrami-Kolmogorov) theory, two nucleation modes are distinguished (Ref 24, 25). The first is a classical nucleation theory, which assumes the uniform thermodynamic properties of the nucleus and the sharp interface between the nucleus and the parent phase. The second is the non-classical nucleation theory of Cahn and Hilliard, which is based on the gradient thermodynamics.

The classical nucleation models include: (i) the continuous nucleation models, (ii) pre-existing nuclei models, (iii) Avrami nucleation models and (iv) mixed nucleation models. All these models are deterministic, and they are described in (Ref 25). A few decades ago, a stochastic character of nucleation was included in modeling of phase transformations and later, for many years, the JMAK approach based on Poisson statistics has been used. Although a majority of the published papers related to stochastic nucleation deal with the crystallization, still solid state transformations are addressed in some publications (see, e.g., (Ref 26)). Following these ideas, it was assumed that the phase transformations introduce stochastic element in the model. This stochasticity relates to the random character of the nucleation of the new phase. Following the framework of classical nucleation model, in the present work a solution for Poisson nucleation was performed. The deterministic nucleation rate equation was replaced by an equation with a stochastic variable, which accounts for the stochastic character of the nucleation. The parameter $\xi(t_i)$, which represents this stochastic variable, satisfies:

$$P[\xi(t_i) = 0] = \begin{cases} p(t_i) & \text{if } p(t_i) < 1 \\ 1 & \text{otherwise} \end{cases} \quad (\text{Eq 6})$$

$$P[\xi(t_i) = 1] = 1 - P[\xi(t_i) = 0]$$

In Eq 6 $p(t_i)$ is a function, which connects the probability of the nucleation with a state of the material in a current time step. This probability was formulated based on the published information regarding nucleation (Ref 27, 28). As a main framework for considerations, the following assumptions were made:

- The nucleus of a new phase may appear only if the condition for starting a given transformation is met. These conditions for all structural components are listed in Table 2.
- The ferritic transformation cannot start if the pearlitic, bainitic or martensitic transformation has already started, the pearlitic transformation cannot start if the bainitic or martensitic transformation has already started and the bai-

Table 2 Conditions determining the beginning of subsequent transformations, where B_s , M_s —bainite and martensite start temperatures, respectively, a_{25} , a_{31} , a_{32} —coefficients in the model

Transformation	Condition to start
Ferrite	$T < A_{e3}$
Pearlite	$c_\gamma > c_{\gamma\beta}(T)$
Bainite	$T < B_s = a_{25}$
Martensite	$T < M_s = a_{31} - a_{32}c_\gamma$

nitic transformation cannot start if the martensitic transformation has already started.

- The nucleation rate increases when the temperature drops below A_{e3} , A_{e1} and B_s for ferrite, pearlite and bainite transformations, respectively.
- Grain boundaries and shear bands in the deformed material provide privileged locations for nucleation; therefore, the probability of nucleation should increase with a decrease of the austenite grain size and an increase of the dislocation density.

Having in mind this knowledge and assuming Poisson nucleation, the following equations were proposed:

Ferrite

$$p(t_i) = a_1 D^{-a_2} \rho^{a_3} [A_{e3} - T(t)]^{a_4} \Delta t \quad (\text{Eq 7})$$

Pearlite

$$p(t_i) = a_{11} D^{-a_{12}} \rho^{a_{13}} [A_{e1} - T(t_i)]^{a_{14}} \Delta t \quad (\text{Eq 8})$$

Bainite

$$p(t_i) = a_{21} D^{-a_{22}} \rho^{a_{23}} [a_{25} - T(t_i)]^{a_{24}} \Delta t \quad (\text{Eq 9})$$

where D is the austenite grain size, ρ is the dislocation density, a_1 , a_2 , a_3 , a_4 , a_{11} , a_{12} , a_{13} , a_{14} , a_{21} , a_{22} , a_{23} , a_{24} , a_{25} —coefficients.

In each time step of calculations Δt , a random number within the range $[0, 1]$ is drawn and compared with the probability $p(t_i)$. If the value of the function $p(t_i)$ in the given time step is greater than the drawn random number, according to Eq 6 the parameter $\zeta(t_i) = 0$ and the new nucleus appears. In the case of martensite, it was assumed that this transformation occurs when the temperature drops below the M_s temperature and the random number is not generated. However, according to Table 2, M_s depends on the carbon content in the austenite, which, in turn, depends on the progress of earlier transformations, see Eq. 3. In consequence, the stochastic component is indirectly introduced into the martensitic transformation.

It should be highlighted that in Eqs. 7-9, the grain size and the dislocation density are stochastic variables (in the form of histograms), which are calculated by the hot forming model described in (Ref 13). Their distribution, however, is determined at the beginning of Eqs. 7-9 and it does not change with time.

3.3 Kinetics of Transformations

After a nucleus of a new phase appears, it starts to grow until another transformation begins or until all phases excluding austenite occupy the whole volume, which marks the end of the

simulation. It was assumed that phase growth in the model is deterministic in nature, which corresponds to the real phase growth process. In order to avoid problems, which occur when the temperature varies during the process, the Leblond differential evolution equation with respect to time (Ref 29) was selected. This equation does not need an application of the additivity rule, what is an important advantage. In this approach the rate of the transformation is proportional to the distance from the thermodynamic equilibrium in a given temperature:

$$\frac{dX(t)}{dt} = k(X(t) - X_{eq}(T(t))) \quad (\text{Eq 10})$$

where t —time, k —coefficient (at the temperature T), $X(t)$ —current volume fraction of a new phase, $X_{eq}(T(t))$ —equilibrium volume fraction of the new phase at the temperature T , which for each phase is provided in Table 2.

Equation 10 is solved using the explicit Euler method:

$$X(t_i) = X(t_{i-1}) + k(T(t_i))(X_{eq}(T(t_i)) - X(t_{i-1}))\Delta t \quad (\text{Eq 11})$$

where Δt —time increment.

Coefficient $k(T(t_i))$ in Eq 11 is a function that depends on several factors, which are constant for the entire simulation, and on the temperature changing over time. As it has been originally shown in (Ref 29), Eq 11 describes well kinetics of the diffusive transformations of ferrite and pearlite. In the case of the bainite, displacive mechanism of the growth has to be considered (Ref 30). When the parameter k_b is properly defined, Eq 11 is able to describe properly displacive growth, as well. The formulas for function k for each transformation are as follows:

Ferrite

$$k_f(T(t_i)) = \frac{a_6}{D^{a_{10}}} \exp\left(-\left(\frac{|T(t_i) - a_7|}{a_8}\right)^{a_9}\right) \quad (\text{Eq 12})$$

Pearlite

$$k_p(T(t_i)) = \frac{a_{16}}{D^{a_{20}}} \exp\left(-\left(\frac{|T(t_i) - a_{17}|}{a_{18}}\right)^{a_{19}}\right) \quad (\text{Eq 13})$$

Bainite

$$k_b(T(t_i)) = \frac{a_{26}}{D^{a_{30}}} \exp\left(-\left(\frac{|T(t_i) - a_{27}|}{a_{28}}\right)^{a_{29}}\right) \quad (\text{Eq 14})$$

Volume fraction $X(t_i)$ in Eq 11 is calculated with respect to the maximum volume fraction of the considered phase at the temperature $T(t_i)$, whereas the final result of the model calculations is $F(t_i)$, which is the volume fraction of the considered phase with respect to the whole volume. By definition, the equilibrium volume fraction X_{eq} is nonnegative and bounded from the above by 1. Thus, $X(t_i)$ for each phase is within a range $[0, 1]$. It is worth mentioning that by the definition, the sum of $F(t_i)$ of all phases equals 1, because it corresponds to occupancy of the whole volume of the sample (see Table 3). As it has been mentioned, grains grow until another transformation starts or until all phases, excluding austenite, occupy the whole volume. In the case of the martensite, it is assumed that this phase occupies the whole volume of the austenite, which remained after preceding transformations at the temperature M_s . Recall, that formulas describing equilibrium volume fractions X_{eq} in Eq 11 and volume fractions F for each phase are listed in Table 3. In this table $F_{fmax}(T)$ is the equilibrium volume fraction of the ferrite at

Table 3 Formulae describing equilibrium volume fractions X_{eq} in Eq 11 and volume fractions F for each phase

Transformation	Equilibrium volume fraction	Volume fraction with respect to the whole volume
Ferrite	$\left. \begin{aligned} X_{eq}(T) &= \frac{F_{f \max}(T)}{F_{eut}} \\ F_{f \max}(T) &= \frac{c_{\gamma 2}(T) - c_0}{c_{\gamma 2}(T) - c_{\gamma}} \end{aligned} \right\} \text{ for } T > A_{e1}$	$F_f(T) = X_f(T)F_{eut}(T)$
Pearlite	$X_{eq}(T) = X_{eut} = 1 \text{ for } T \leq A_{e1}$	$F_p(T) = X_p(T)(1 - F_f(T))$
Bainite	$X_{eq}(T) = 1$	$F_b(T) = X_b(T)(1 - F_f(T) - F_p(T))$
Martensite		$F_m(T) = 1 - F_f(T) - F_p(T) - F_b(T)$

the temperature T . Maximum ferrite volume fraction in steel is equal to the equilibrium ferrite volume fraction at the eutectic point F_{eut} , which is defined by Eq 5.

In the developed model coefficients a_1, \dots, a_{32} are determined by the inverse analysis for the experimental data. The model with optimized coefficients predicts distributions of volume fractions of phases. These parameters will be used to predict local gradients of properties, which influence formability (Ref 31).

Numerical tests, which evaluated an influence of selected numerical parameters used in the model on the accuracy and the computation time of simulations, were already conducted in previous paper (Ref 23). The following issues were investigated in relation to their influence on the reliability of results of numerical experiments: (i) type of the random number generator (RNG), (ii) maximum time step and temperature change during the time step, (iii) sufficient number of the Monte Carlo (MC) points. The optimal values of these parameters were proposed having in mind a balance between accuracy and computing times. On the basis of these tests, it was concluded that:

- The model result does not depend on a random number generator, which was used.
- Setting the maximum temperature change per step to 0.1 °C and the maximum time change per step to 0.5 s results in a good balance between accuracy and computing costs.
- Outputs of simulations are stable (i.e., the simulation result is not too random) above 10000 MC points. Moreover, performing the simulation for more MC points does not ensure that the result is better, but it increases the computational cost.

4. Sensitivity Analysis and Uncertainty of the Stochastic Model Identification

The sensitivity analysis (SA) (Ref 32, 33) preceded the inverse analysis with the objective to evaluate importance of the coefficients in the stochastic model and to find the coefficients which influence the output most. The effect of the change of the j th coefficient (Δa_j) on the model output is:

For the average output parameters:

$$\chi_j(\mathbf{a}) = \frac{a_j y(a_1, \dots, a_{j-1}, a_j + \Delta a_j, a_{j+1}, \dots, a_k) - y(\mathbf{a})}{\Delta a_j y(\mathbf{a})} \quad (\text{Eq 15})$$

For the output histograms:

$$\chi_j(\mathbf{a}) = a_j \frac{d(H_1, H_2)}{\Delta a_j} \quad (\text{Eq 16})$$

where χ_j —the sensitivity factor for the j th coefficient, Δa_j —an increment of the j th coefficient, $y(\mathbf{a})$ —output of the model in the form of average values of parameters, H_1 —the basic histogram calculated for the coefficients \mathbf{a} , H_2 —histogram obtained after disturbance of the coefficient a_j by Δa_j , k —number of coefficients in the model.

The distance between histograms H_1 and H_2 in Eq. 16 is measured using the earth mover’s distance (EMD), which is defined by the formula (see (Ref 34)):

$$\text{EMD} = \sum_{m=1}^n |\text{EMD}_m| \quad \text{EMD}_m = \sum_{l=1}^m [H_1(l) - H_2(l)] \quad (\text{Eq 17})$$

where n —the number of bins in the histogram.

All calculations for the output in the form of average values of parameters were performed for the forward and backward finite difference quotients. Since similar sensitivity factors were obtained for different quotients, the results for the forward finite difference quotient only (Eq 15) are presented.

The Monte Carlo method with 10000 MC points was used in simulations. Since the model is stochastic, the result can be different for each simulation run even for the same set of coefficients. Thus, the SA can state that there is an influence of some coefficients even if the result did not significantly change. To improve the SA, it was decided to filter this, “stochastic noise” by discarding the cases, in which the change of the output is below a certain threshold ($\chi_j = 0$ was assumed). On the basis of the numerical tests performed in (Ref 23), the threshold of 2 °C for temperatures and 0.004 for volume fractions was used.

The primary SA for the model was performed in (Ref 23) assuming $\Delta a_j = 0.1a_j$. However, due to a mutual interrelation between transformations, a non-physical influence of the coefficients was sometimes observed for such large increments Δa_j . Thus, in the present paper it was decided to evaluate the influence of the coefficients increments on the SA results and calculations for increments 10%, 5%, 3% and 1% of a_j were

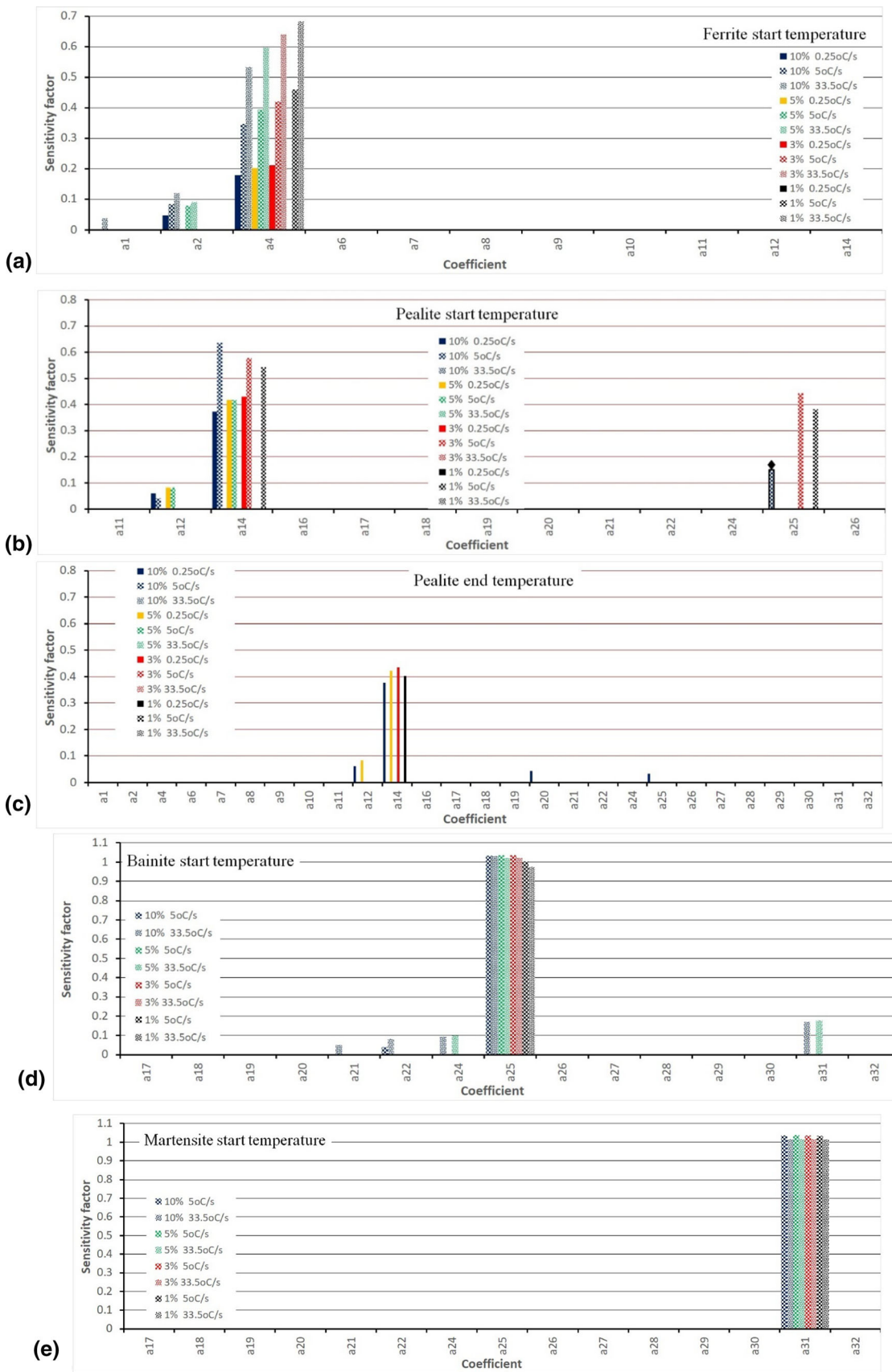


Fig. 1 Sensitivity Analysis (SA): influence of the model coefficients on the start temperatures of ferrite (a) pearlite (b), bainite (d) and martensite (e) and pearlite end temperature (c) for various increments Δt_i in Eq 15 and for various cooling rates

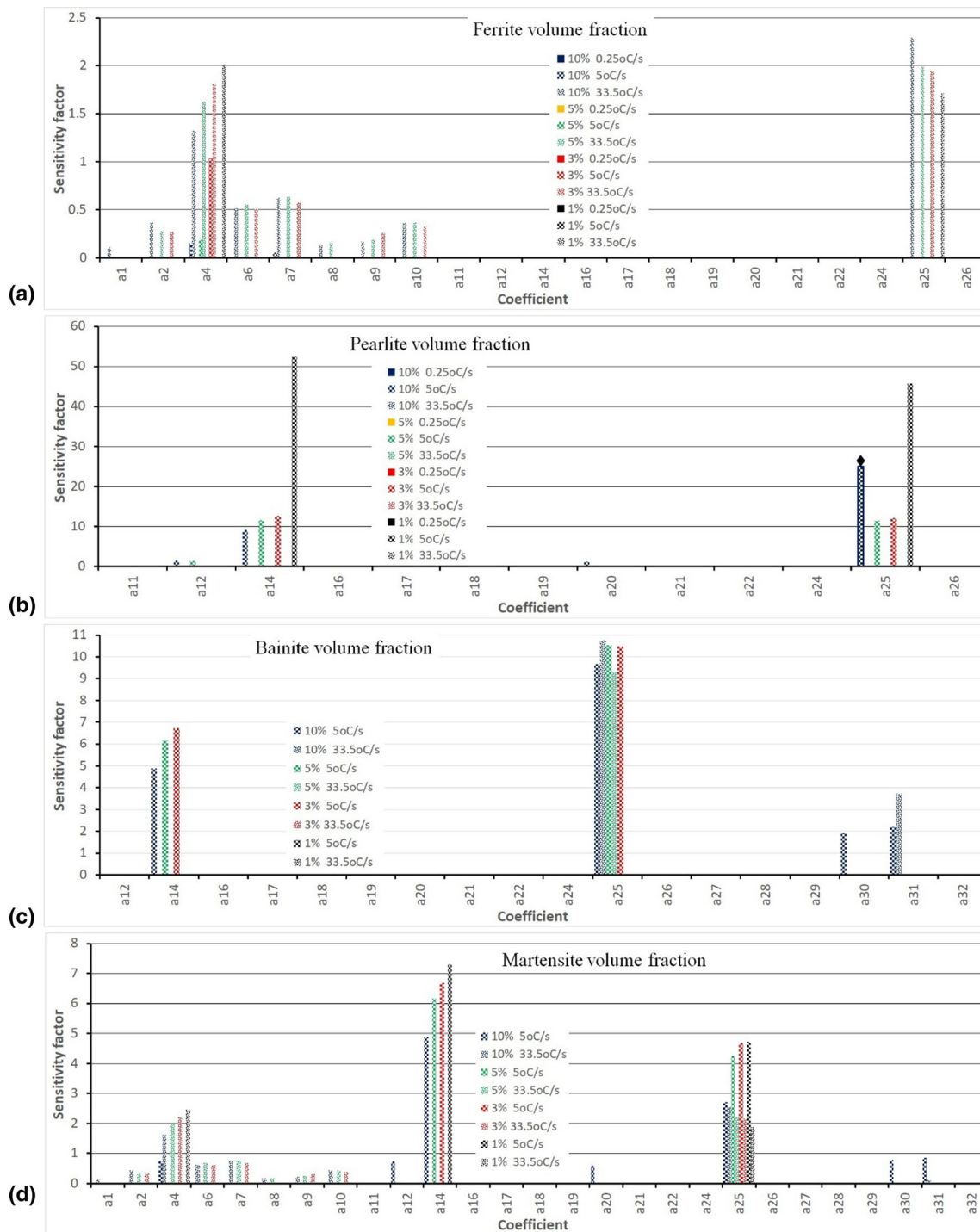


Fig. 2 Sensitivity Analysis (SA): influence of the model coefficients on the average volume fractions of ferrite (a), pearlite (b), bainite (c) and martensite (d) for various increments Δa_j in Eq 15 and for various cooling rates

performed. The coefficients a_3 , a_{13} and a_{23} were not considered because they are responsible for the influence of a dislocation density, which is not yet taken into account in the cooling model. The coefficients a_5 and a_{15} were not considered either, because currently they do not appear in the model. The temperature of the end of bainite transformation was not considered because it has not appeared in the experiments for the investigated steel. The SA was performed for the three cooling rates: 0.25 °C/s, 5 °C/s and 33.5 °C/s, and the results

are shown in Fig. 1, 2 and 3. Since bainite and martensite do not occur for the cooling rate of 0.25 °C/s, these results are omitted, as well. Absolute values of the sensitivity factors are presented in the figures.

During the SA, specific cases were observed, in which a change of the coefficient a_j by Δa_j resulted in a situation that the transformation which occurred for the original set of coefficients disappeared or vice versa. It happened for the coefficient a_{14} (a decrease by 10% and 5% resulted in disappearing of the pearlite)

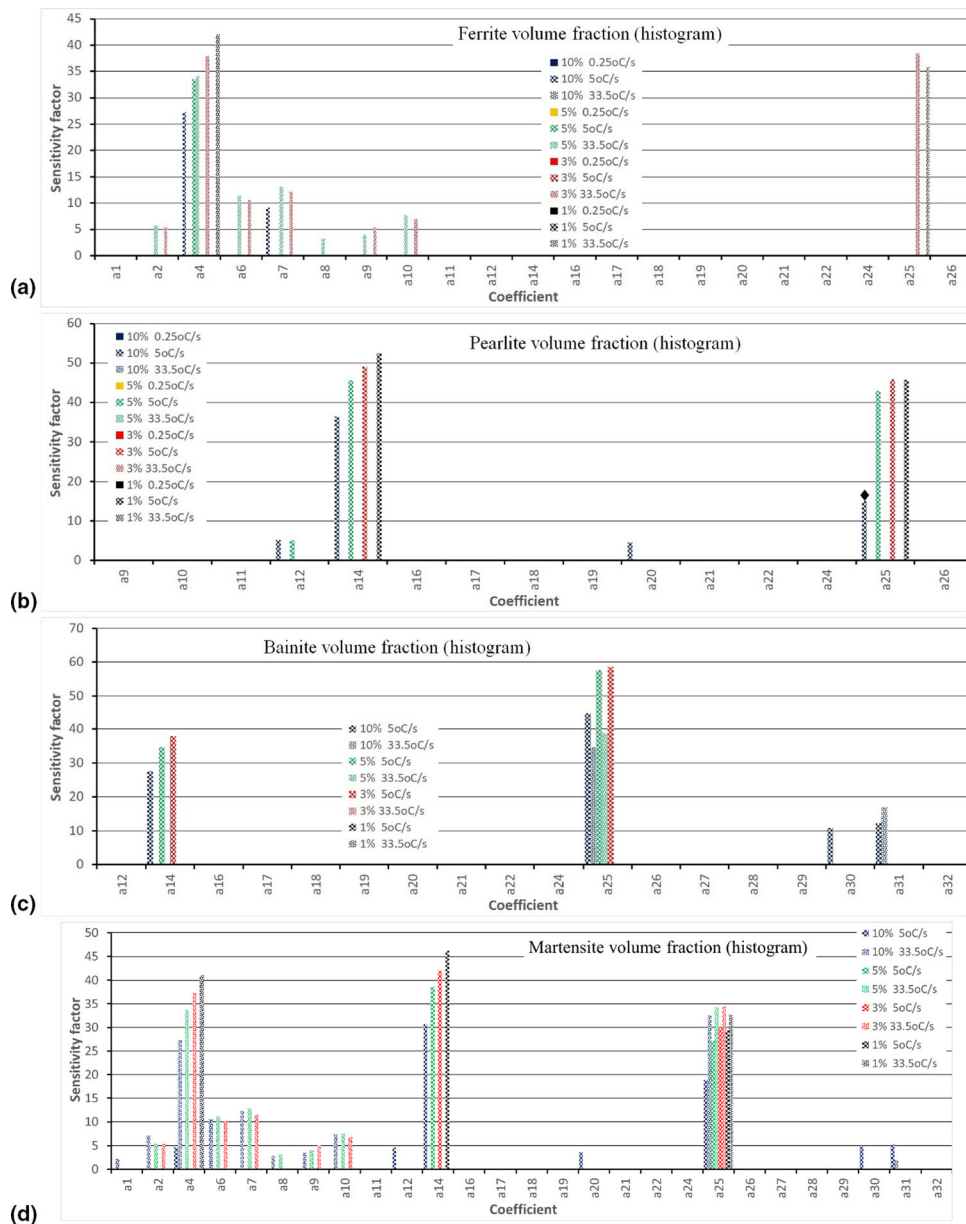


Fig. 3 Sensitivity Analysis (SA): influence of the model coefficients on the histograms of the volume fractions of ferrite (a), pearlite (b), bainite (c) and martensite (d) for various increments Δa_j in Eq 16 and for various cooling rates

and for the coefficient a_{25} (an increase by 10% resulted in disappearing of the pearlite). The sensitivity factor could not be calculated for this qualitative change of the output, and these cases were marked with a bar surrounded by a line and with a symbol \blacklozenge . The length of this bar has no meaning. This disappearing and appearing of the transformation can cause difficulties in the coefficients identification.

The analysis of the results of the SA brought the conclusion that for the simulation result the most crucial coefficients are a_4 , a_{14} , a_{25} and a_{31} . The following coefficients have the biggest impact on the individual output parameters:

- Ferrite temperature start: a_4
- Pearlite temperature start: a_{14} , a_{25}
- Pearlite temperature end: a_{14}
- Bainite temperature start: a_{25}
- Martensite temperature start: a_{31}

- Ferrite volume fraction: a_4 , a_6 , a_7 , a_{25}
- Pearlite volume fraction: a_{14} , a_{25}
- Bainite volume fraction: a_{14} , a_{25} , a_{31}
- Martensite volume fraction: a_4 , a_6 , a_7 , a_{14} , a_{25} , a_{31}

Coefficients a_1 , a_2 , ..., a_9 , a_{10} appear in the ferrite transformation in the model, coefficients a_{11} , a_{12} , ..., a_{19} , a_{20} in the pearlite transformation, coefficients a_{21} , a_{22} , ..., a_{29} , a_{30} in the bainite transformation, and coefficients a_{31} and a_{32} in the martensite transformation. It is clear that changes in coefficients may significantly influence respective temperature or volume fraction in the model output. However, as was revealed by the SA, the coefficients that appear in one transformation can influence the volume fraction of other phase as well. Since the volume fractions of all phases sum up to 1, if one phase takes significantly more/less volume (because of an earlier/later start of the transformation or a faster/slower growth of the phase), it

will also affect other phases. That change in the volume does not affect the temperatures of start of the transformations though—in Fig. 1 it is clearly seen that the only influence on the temperatures comes from the coefficients that appear in the respective transformation. However, there can be exceptions to that, because when one transformation begins much earlier, it can result in not starting the previous transformation, in consequence in some MC points this transformation does not occur at all and that has influence on the average temperature—in the described SA it happened in the case of the coefficients a_{25} and a_{31} . Their change caused that, respectively, pearlitic or bainitic transformation did not occur for some MC points. This can affect more than one temperature, e.g., if Δa_{25} is large, it causes that even the ferritic transformation may not occur in some MC points. Similarly, when some coefficients, e.g., a_{25} , are lowered, it can result in starting a previous transformation in some MC points even if without a coefficient change that transformation would not appear at all in these MC points.

Other important conclusions from this SA are: (a) the change of the coefficients affects volume fractions relatively much more than the temperatures, (b) with low cooling speed the change of the coefficients does not affect the result much, compared to the other cooling speeds—less coefficients can change the result significantly and the influence is lower, (c) the coefficients that affect the simulation result the most are the ones responsible for starting of a transformation, and not the ones responsible for the growth of a phase.

The smallest Δa_j (with a 0.01% accuracy), for which any coefficient change does not affect the simulation result, was also found. This happens for Δa_j equal $0.0033a_j$. From $\Delta a_j = 0.01a_j$ downwards, there is only influence of the coefficients a_4, a_{14}, a_{25} and a_{31} . However, several coefficients (ie. $a_1, a_{11}, a_{16}, a_{17}, a_{18}, a_{19}, a_{21}, a_{26}, a_{27}, a_{28}, a_{29}, a_{30}, a_{32}$) can be changed by $0.05a_j$ without influencing the simulation result.

The SA determined the model coefficients, which contribute the most to the model output and those, which are not significant (Ref 35). The SA results were used as a support for the design of the optimization strategy in the inverse analysis.

5. Identification of the Coefficients in the Stochastic Model

The stochastic model of phase transformations contains several coefficients, which must be determined for each specific material. In general, these are fitting coefficients, which allow to reproduce the experimental data. Some of these coefficients have a physical meaning but they still have to be determined for each investigated steel. Identification of the coefficients is performed using inverse analysis for the experimental data. These data contain both measurements of the average transformation temperatures and measurements of histograms of phase volume fractions.

5.1 Formulation of the Inverse Problem for the Stochastic Experimental Data

The problem of the identification of the coefficients in material models is widely discussed in the scientific literature as the inverse problem (Ref 36-38). The algorithm for the stochastic inverse problem is described in (Ref 39). Inverse

approach is transferred into an optimization task with the coefficients \mathbf{a} becoming the state variables and the following objective function:

$$\Phi(\mathbf{a}) = d(y_c(\mathbf{a}), y_m) \quad (\text{Eq 18})$$

where $y_c(\mathbf{a})$ —outputs calculated for the model coefficients \mathbf{a} , y_m —measurements in the experimental tests, d —metric in the output space Y .

In earlier paper (Ref 12), the optimization task was redefined for the stochastic variable model. Since the output of the stochastic model is in the form of histograms, the metric d in Eq 16 had to take into account that the random variable $\xi(t_i)$ in the Eq 6 and stochastic nature of D and ρ (input parameters for the model) can lead to different single solutions for the same starting values. Similarly, as it was done in the sensitivity analysis (Sect. 4), EMD was used as the measure of the distance between calculated ($H_c(\mathbf{a})$) and measured (H_m) histograms. To be able to apply EMD metric (Eq 17), the experimental data should include information on distributions of the temperatures of phase transformations and phase fractions. Since the measurement of histograms of these temperatures is not physical, it was decided to compare only histograms of phase fractions and average start and end temperatures of transformations. Thus, the objective function (Eq 18) was reformulated to a hybrid form as follows:

$$\Phi(\mathbf{a}) = \Phi_T(\mathbf{a}) + \Phi_F(\mathbf{a}) \quad (\text{Eq 19})$$

The components of the objective function are calculated as follows. The component $\Phi_T(\mathbf{a})$ is the sum of the mean square root errors (MSRE) between measured and calculated average start/end temperatures of transformations:

$$\Phi_T(\mathbf{a}) = \sqrt{\frac{1}{Ne} \sum_{i=1}^{Ne} \left(\frac{w_T}{Nt_i} \sum_{j=1}^{Nt_i} \left(\frac{T_{ij}^m - T_{ij}^c(\mathbf{a})}{T_{ij}^m} \right)^2 \right)} \quad (\text{Eq 20})$$

The component $\Phi_F(\mathbf{a})$ is the sum of the EMDs (Eq 17) between measured and calculated histograms of the phase volume fractions after cooling:

$$\Phi_F(\mathbf{a}) = \sum_{i=1}^{Ne} \left(\frac{w_F}{Nf_i} \sum_{j=1}^{Nf_i} \text{EMD}(H_{ij}^m, H_{ij}^c(\mathbf{a})) \right) \quad (\text{Eq 21})$$

where $T^c(\mathbf{a})$ —average value of the start/end temperature of transformation calculated for model coefficients \mathbf{a} , T^m —the average start/end temperature of transformation determined from the dilatometric tests (Ref 24), H^m —distribution (histogram) of the phase fraction measured in the dilatometric tests, $H^c(\mathbf{a})$ —distribution (histogram) of the phase fraction calculated by the model with coefficients \mathbf{a} . Superscripts m and c refer to measurement and calculations, respectively.

5.2 Optimization with the Objective Function Based on the Measured and Calculated Average Values of Microstructural Parameters

In the case of the inverse analysis carried out in this work, the coefficients $\mathbf{a} = \{a_1, \dots, a_{32}\}^T$ for the analyzed stochastic model of phase transformations have to be determined. As it is seen in Sect. 3, the coefficients \mathbf{a} directly influence modeling of the cooling of the steel components after hot forming. In this process, the model predicts the start and end temperature of phase transformations (T) and volume fractions of structural

components (F) after cooling. The inverse analysis described in Sect. 5.1 was used to determine coefficients of the model based on the experimental data.

5.2.1 Experiment. The material used in the experiments was the steel containing 0.12%C and 1.3%Mn and 0.05%Si (Ref 24). The experiments composed dilatometric tests performed with cooling rates in the range 0.1 – 100 °C/s. Two austenitization temperatures were used (1080 °C and 1150 °C), and in consequence, two austenite grain sizes prior to transformations were obtained (17 and 24 μm). The austenitization time was 120 min in every test. The experimental data, which are available now, provided information on the transformation temperatures, as well as volume fractions of the structural components for different austenite grain size prior to transformations. Thus, the primary objective of the work was the identification of the model coefficients for the average values of the output parameters. At this stage, there were not available experimental data for the non-recrystallized austenite and the effect of the dislocation density prior to transformations could not be evaluated. Thus the coefficients a_3 , a_{13} and a_{23} were assumed zero, which is adequate for the recrystallized austenite.

5.2.2 Definition of the Objective Function. The correct definition of the objective function is crucial for the quality of the optimization. At this stage of the project, the histograms of the output parameters are not measured. Therefore, the objective function based on measurements of the average values (instead of histograms) of transformation temperatures and phase volume fractions was proposed. Consequently, in Eq 21 the term with EMDs was substituted by the root mean squared error (RMSE) between measured and calculated average phase volume fractions and then combined with Eq 20. Finally, the following objective function was proposed:

$$\Phi(\mathbf{a}) = \sqrt{\frac{1}{Ne} \sum_{i=1}^{Ne} \left(\frac{w_T}{Nt_i} \sum_{j=1}^{Nt_i} \left(\frac{T_{ij}^m - T_{ij}^c(\mathbf{a})}{T_{ij}^m} \right)^2 + \frac{w_F}{Nf_i} \sum_{k=1}^{Nf_i} (F_{ik}^m - F_{ik}^c(\mathbf{a}))^2 \right)} \quad (\text{Eq 22})$$

where Ne —number of the tests, Nt_i —number of the temperature measurements in the i th test, Nf_i —number of the average phase volume fractions measured in the i th test, T —start or end temperature of the phase transformation, F —phase volume fraction after cooling, w_T , w_F —weights for temperatures and phase volume fractions, respectively. Superscripts m and c refer to measurements and calculations, respectively.

Since volume fractions of phases by definition are in the range $[0,1]$, the square of the difference between measured and calculated values of F in Eq 22 is not divided by the measured value.

5.2.3 Selection of Weights for Objective Function. Since absolute values of temperatures and phase volume fractions differ significantly, their influence on the objective function has different range. Thus, a selection of weights in Eq 22 is important. The weights have no physical meaning, they decide about the contribution of the temperatures and the phase volume fractions to the objective function. The sum of the weights should be equal 1. In the first approach, the weights $w_T = 0.5$ and $w_F = 0.5$ were used. The objective function $\Phi = 0.346$ was obtained. However, evaluation of the obtained results indicated that a more accurate solution for the average volume fractions would be possible if larger weights were used

for the volume fractions and smaller weights for temperatures. After the tests, it was decided to use $w_T = 0.1$ and $w_F = 0.9$. This resulted in more accurate results for volume fractions, at the expense of a small loss in the accuracy for temperatures. The lowest value of the objective function obtained after changing the weights was $\Phi = 0.114$. By using the objective function (20), it was possible to determine the model coefficients for the analyzed steel.

5.2.4 Selection of the Optimization Method. To accomplish this task, several optimization algorithms were tested, including the most promising global heuristic optimization methods. Population-based algorithms are now commonly used in various applications. The particle swarm optimization (PSO), which was successfully applied to identification of the stochastic hot forming model (Ref 12), was selected for all subsequent optimizations in the present work.

5.2.5 Emerging Problems in Optimization. The main problem in the identification of the phase transformation models is the large number of coefficients. The local minima, which are due to strong dependencies between the models of individual phase transformations, are another difficulty. The next problem is finding solutions for all coefficients with wide ranges, where even the smallest changes in the coefficients generate significant changes in the model response, as shown by the SA in Chapter 4.

It has already been shown in publication (Ref 40) that connections between the models of individual phase transformations do not allow to identify the transformation models independently. Improving the model of one transformation very often resulted in a deterioration of the transformation model of another phase. Therefore, it is necessary to perform optimization on all coefficients simultaneously for the result to be reliable and stable. With deterministic models, researchers have already struggled to solve problems with a very large number of local minima when using inverse analysis. The optimization was divided into separate steps using a multistage approach. In the first step, the coefficients responsible for the successive start/end temperatures of phase transformations and the phase volume fractions were optimized separately in the following groups: ferrite start temperature (a_1, a_2, a_3, a_4), pearlite start temperature ($a_{11}, a_{12}, a_{13}, a_{14}$), bainite start temperature ($a_{21}, a_{22}, a_{23}, a_{24}, a_{25}$), martensite start temperature (a_{31}, a_{32}), ferrite volume fraction ($a_6, a_7, a_8, a_9, a_{10}$), pearlite volume fraction ($a_{16}, a_{17}, a_{18}, a_{19}, a_{20}$) and bainite volume fraction ($a_{26}, a_{27}, a_{28}, a_{29}, a_{30}$). This allowed for the initial detection of optimal ranges for coefficients. Initial narrowing of the ranges for the coefficients resulted in a much lower objective function when optimizing on all coefficients. The best results were achieved by a strategy that used knowledge about the best individuals from the population from previous optimizations in a multistage approach.

5.2.6 Results of Optimization on Average Values. The optimal coefficients obtained during inverse analysis for the average experimental data are presented in Table 4. The graphs showing comparison of measured and calculated transformation temperatures and phase volume fractions are presented in Fig. 4. In this figure F , P , B and M refer to ferrite, pearlite, bainite and martensite and indices s and e refer to start and end temperatures of transformations.

Table 4 Optimal values of the coefficients in the model

a_1	a_2	a_3	a_4	a_5	a_6	a_7	a_8	a_9	a_{10}	a_{11}
3.71×10^{09}	1.432	0	4.881	0	0.606	795.17	710.53	0.8866	0.2391	3.88×10^{11}
a_{12}	a_{13}	a_{14}	a_{15}	a_{16}	a_{17}	a_{18}	a_{19}	a_{20}	a_{21}	a_{22}
0.8998	0	4.9507	0	0.4562	567.91	535.16	1.8509	0.6296	0.3513	0.5274
a_{23}	a_{24}	a_{25}	a_{26}	a_{27}	a_{28}	a_{29}	a_{30}	a_{31}	a_{32}	
0	0.4826	546.24	0.1708	576.5	781.42	0.8484	0.8808	393.86	24.717	

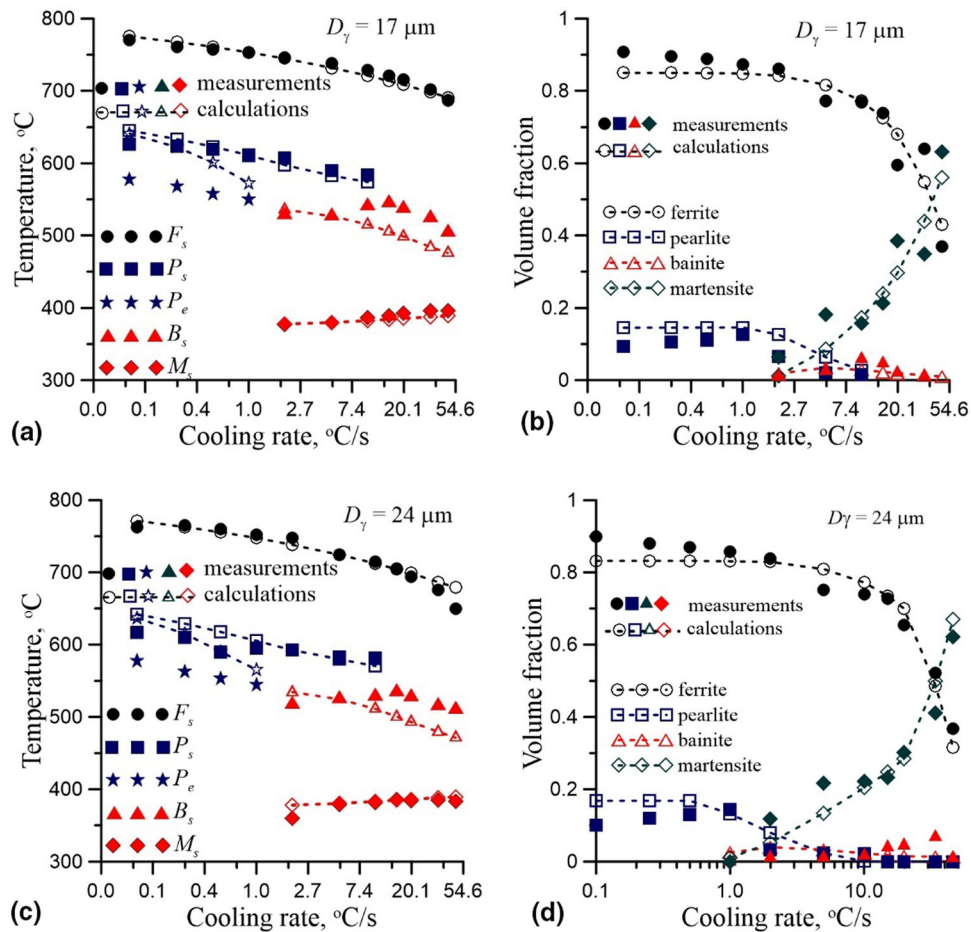


Fig. 4 Comparison of the measured and calculated for the optimal coefficients temperatures of phase transformations (a, c) and volume fractions of structural components (b, d), austenite grain size prior to transformations $17 \mu\text{m}$ (a, b) and $24 \mu\text{m}$ (c, d)

6. Numerical Tests of the Inverse Analysis for the Stochastic Experimental Data

Inverse analysis for the measured microstructure parameters in the form of histograms allows for a more accurate identification of the model coefficients by using the entire available frequency distribution. However, this also translates into a much higher computational effort and thus a much longer optimization.

6.1 Formulation of the Inverse Problem

As it has been mentioned in the previous chapter, at this stage of the project the measurements of histograms of the output parameters are not available. The objective of numerical tests described in this chapter was to evaluate capability of the inverse analysis to determine coefficients in the model when such measurements of the histograms are available. Thus, the histograms of phase volume fractions were calculated using the model with the coefficients in Table 4 and these histograms were considered as experimental data. Following this, the values of the coefficients were randomly perturbed and optimization was performed.

The optimization was performed for the objective function (Eq 19), which is a successive summing of the square root errors between measured and calculated transformations tem-

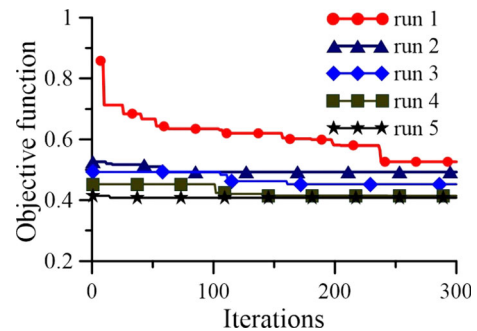


Fig. 5 Decrease of the objective function in subsequent optimization runs when the best individuals are remembered

peratures and metrics of the distance between the measured and calculated histograms of the phase volume fractions. The Earth Mover's Distance (EMD) defined by the Eq 17 was selected as the latter metrics.

6.2 Discussion of the Optimization Problems and Results

6.2.1 Emerging Problems in Optimization for the Stochastic Experimental Data. The main problems in identification of the stochastic phase transformation models are similar to those discussed in Sect. 5.2 for the optimization

based on measurements of average values of microstructural parameters. However, in the case of a stochastic model, where the number of model calls corresponds to the number of Monte Carlo (MC) points used, these problems generate a huge computational effort and the probability of obtaining a local minimum is higher. The local solution in most cases generates incorrect coefficients for a given model.

6.2.2 Proposed Solutions to Emerging Problems. It was decided to solve the problem related to the high number of optimized coefficients by using cascade models and optimizing each phase separately. This approach allowed for the initial narrowing of the ranges for the coefficients and, based on them, the creation of attractive individuals for optimization for all

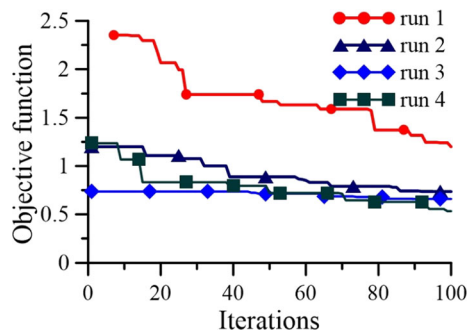


Fig. 6 Decrease of the objective function depending on the optimization strategy

phases simultaneously. The problem of occurrence and getting stuck in local minima was solved by using multiple optimization runs with a new population, whenever the optimization stops at one point for a long time. The selection of Monte Carlo points for optimization was based on the results of the solution stability tests and is described in more detail later in the article. The optimization strategy for effective identification takes into account results of the sensitivity analysis. The approach used allows for a significant reduction in the search space for coefficients, which translates into shorter calculation time and better results.

The analyses indicated that the best strategy was based on partial optimizations for each phase, which indicated the ranges for coefficients where good solutions occurred. These ranges were then used to optimize on all coefficients simultaneously. For subsequent optimization runs, sets of coefficients that generated good solutions were added to the new population in order to search their neighborhoods.

6.2.3 Adjusting the Optimization Ranges. For some coefficients, the model output was extremely sensitive to even their small changes. This was important for the coefficients a_1 and a_{11} , which had values with a high degree of decimal accuracy. In order to eliminate this phenomenon, a range of updating mechanism was used. After a certain number of iterations, recorded the data of the best individual from the population and then updated the ranges for optimization. This approach allowed for excluding ranges where the solutions generated the large objective function, and then slowly approaching the appropriate values for the coefficients.

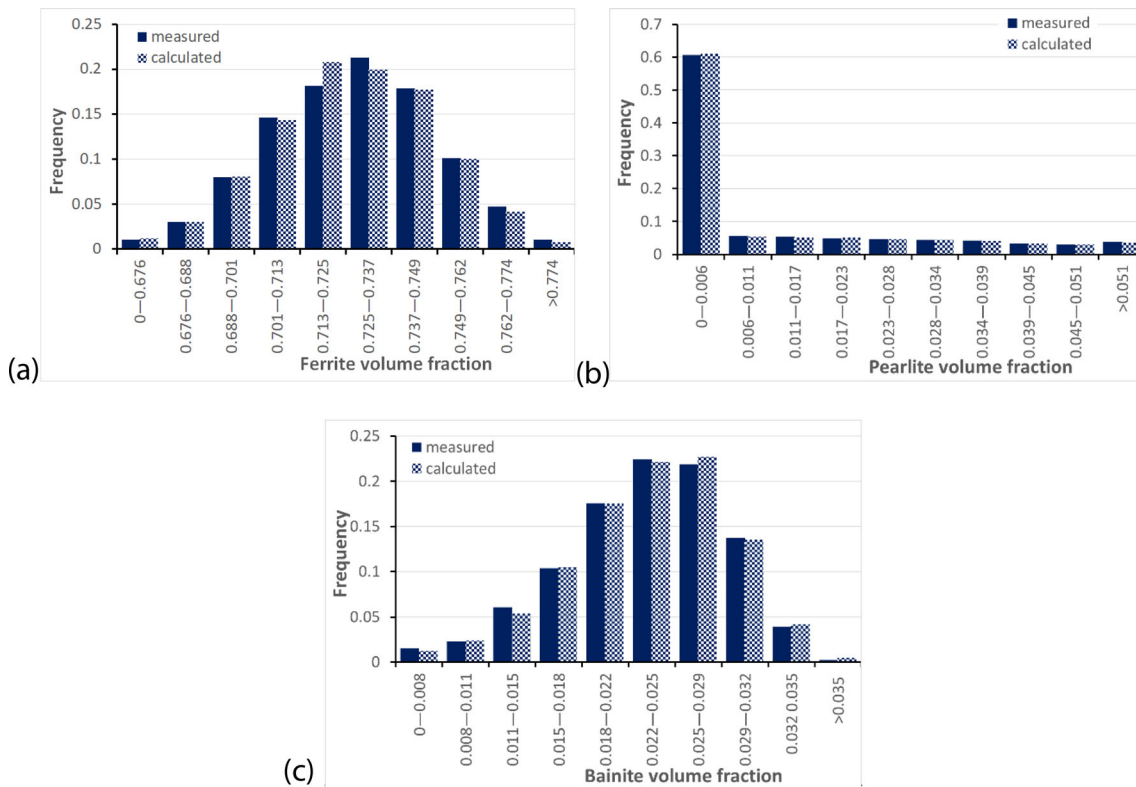


Fig. 7 Selected examples of comparison of measured and calculated histograms of the volume fractions of ferrite (a), pearlite (b) and bainite (c) for the cooling rate of 15 °C/s

6.2.4 Selecting the Number of Monte Carlo Points for Optimization. The number of MC points was another particularly important problem in the optimization. It was proved in (Ref 23) that the model is stable at the level of 10,000 points. When optimizing for all coefficients, using such a large number of MC points is inefficient. Almost the whole time is used on calculations performed for combinations of coefficients that are very far from the best solution. A solution in this case may be a cascade approach to identify model coefficients (Ref 41).

For temperatures, it was decided to adopt values that do not exceed 1 °C of difference between two subsequent model calls. For volume fractions, it was decided to adopt values that do not exceed $EMD = 0.1$ between two consecutive model calls. Following the above-mentioned rule, it was decided to adopt 4000 points for the starting temperature of the ferritic and the pearlitic transformation, 2000 points for the starting temperature of the bainitic transformation, and 1000 points for the starting temperature of the martensitic transformation. For volume fractions, the stability was achieved for 2000 points for ferrite, 4000 points for pearlite and 1500 points for a bainite. This approach significantly reduced the computational cost of optimization while maintaining satisfactory accuracy of results.

Optimization for all phase transformations was performed for 10000 MC points, and good accuracy was obtained. This was due to the fact that ranges of occurrence of valuable solutions or coefficients that well reflected individual phases during partial optimizations have already been available.

6.2.5 Performing Partial Optimizations. During partial optimizations, a predetermined number of MC points was used, based on research on the stability of model solutions for individual phases. The generated solutions for three process parameters were placed in histograms containing 10 bins. In order to reduce the required number of calculations, it was decided to limit the number of used different cooling rates tests to seven, selecting those that are the most important, as they are located on the edges of the occurrence of the phase transformations.

In the PSO, a population of 24 individuals was used. The number of optimization runs depended on whether the value of the objective function achieved better values after subsequent optimization runs. If it decreased, it was possible to update the ranges. If not, the partial optimizations for a given parameter were completed. This approach allowed to determine the ranges for the coefficients for all temperatures and volume fractions, respectively. With global optimization using wide ranges, achieving such low values would be problematic and extremely time-consuming due to the high number of coefficient combinations and the wide occurrence of local minima. The current approach found ranges where there should be mostly good solutions for a given parameter.

6.2.6 Optimization for All Phase Transformations. After obtaining the coefficients for each parameter separately, it was possible to determine the ranges for optimization for all phase transformations. It was possible to configure a set of coefficients consisting of the best ones found from the partial optimizations. The created set of coefficients allowed to start optimization with an individual in the population that well reproduced the experimental data for individual phases.

An important issue when creating ranges for coefficients around the best points was how much to increase/decrease the coefficients for such optimization. For the purposes of present

research, it was decided to examine the neighborhood of the best coefficients found during partial optimizations, perturbing the best coefficients by 10% and taking these values as the minimum and maximum ranges for the coefficients.

To test the capabilities of the adopted optimization methodology, the tests were carried out on a smaller number of Monte Carlo points and a simplified objective function (only one grain size $D = 17 \mu\text{m}$ was considered). The purpose of these tests was to demonstrate the capabilities of remembering the best individuals from the population. The graph in Fig. 5 shows that the technique of remembering the best individuals from previous optimizations allows subsequent optimizations to start at the point where the previous ones ended. This approach is valuable because the random population generated at the start of each new optimization may contain better individuals.

It was decided to perform optimization on the adopted ranges using 100 iterations. The population was assumed to be eight individuals, and an individual was added to it based on the best coefficients obtained from partial optimizations. 10000 MC points were used during the optimization, which aimed to find a stable and accurate result. A graph showing the decrease of the objective function (17) is presented in Fig. 6. Results for the four following runs are presented: (1) random initial population, (2) random initial population with additional the best individual from the run 1 added, (3) random initial population with additional the best individuals from the runs 1 and 2 added, (4) random initial population with the additional individual created on the basis of the best individuals from the partial optimization added.

The graph shows that there are benefits to the approach of using the best coefficients from partial optimizations and creating an individual from them. This approach allowed to start optimization in proximity to the low local minimum. For comparison, the graph also shows the decrease of the objective function when no additional individual created on the basis of the best coefficients from partial optimizations was used. Then the best individual from this population was added to the next optimization run.

The approach used here seems valuable. By finding sets of coefficients in partial optimizations and then using the best coefficients, it is possible to obtain accurate results. Combined with the technique of remembering the best individuals from each optimization run, this allows the value of the objective function to be improved in each subsequent run. The results obtained during optimization allowed the identification of models with no visual differences comparing to the plots in Fig. 4; therefore, these data are not presented.

Figure 7 shows an example of a comparison between the measured and calculated histograms for the volume fractions of ferrite, pearlite and bainite. The calculated histograms were obtained from the model with coefficients, which gave the lowest value of the objective function (Eq 19). Histograms were generated for 10000 Monte Carlo points. The adoption of such a number resulted from stability studies, where it was established that for such a number the model result becomes stable.

The histograms obtained from the model coincide with those from the experiments. The differences in the histograms are negligible, which also translates into a very low objective function.

7. Conclusions

The stochastic phase transformations model, which accounts for a random character of phase transformations during cooling of steels and calculates distributions (histograms) of microstructural features, was proposed. The numerical tests, with the objective to select the best numerical parameters, were performed, and the following conclusions were drawn:

- (1) The use of a random factor results in generating a diverse output histograms, which allows for the characterization of the heterogeneous microstructures. Beyond this, the model reflects the random nature of a nucleation of a new phase in steel.
- (2) Maximum changes per step were determined as 0.1 °C for temperature and 0.5 s for time. As a result, a good balance between accuracy and computing costs was obtained.
- (3) The simulations were stable when at least 10000 Monte Carlo points were used.
- (4) The sensitivity analysis showed that the volume fractions are much more affected than the temperatures by the coefficients' change, and that the coefficients affect the model less at low cooling rates. The coefficients responsible for starting of transformations influence the model output more than the ones responsible for a growth of phases.
- (5) Optimization on average values allowed the identification of coefficients in the model based on the available measurements at a satisfactory level.
- (6) A hybrid objective function combining MSRE for average values with the Earth Movers Distance (EMD) for histograms allowed for the identification of coefficients, with emphasis on the histograms of the phase volume fractions.
- (7) A multistep approach to the optimization turned out to be an efficient solution. In the first step a preliminary ranges of coefficients, in which good solutions occurred, were determined. The final optimization for the narrow ranges proved valuable in terms of the results obtained.

Funding

This study was funded by the National Science Foundation in Poland (NCN) project 2021/43/B/ST8/01710.

Conflict of interest

Authors declare that they have no conflict of interest.

Ethical Approval

This article does not contain any studies with human participants or animals performed by any of the authors.

Open Access

This article is licensed under a Creative Commons Attribution 4.0 International License, which permits use, sharing, adaptation, distribution and reproduction in any medium or format, as long as

you give appropriate credit to the original author(s) and the source, provide a link to the Creative Commons licence, and indicate if changes were made. The images or other third party material in this article are included in the article's Creative Commons licence, unless indicated otherwise in a credit line to the material. If material is not included in the article's Creative Commons licence and your intended use is not permitted by statutory regulation or exceeds the permitted use, you will need to obtain permission directly from the copyright holder. To view a copy of this licence, visit <http://creativecommons.org/licenses/by/4.0/>.

References

1. J.G. Lenard, M. Pietrzyk and L. Cser, *Mathematical and Physical Simulation of the Properties of Hot Rolled Products*, Elsevier, Amsterdam, 1999
2. J. Furstoss, M. Bernacki, C. Petit, J. Fausty, D.P. Munoz and C. Ganino, Full Field and Mean Field Modeling of Grain Growth in a Multiphase Material under Dry Conditions: Application to Peridotites, *J. Geophys. Res. Solid Earth*, 2020 <https://doi.org/10.1029/2019JB018138>
3. B. Aktas and C. Simsir, Investigation of Full-Field and Mean-Field Models for Pure Grain Growth Simulations, *Hittite J. Sci. Eng.*, 2021, **8**(1), p 41–47
4. L. Maire, Full Field and Mean Field Modeling of Dynamic and Post-Dynamic Recrystallization in 3D—Application to 304L steel, PhD thesis, MINES ParisTech, 2018
5. Y. Rémond, S. Ahzi, M. Baniassadi and H. Garmestani, *Applied RVE Reconstruction and Homogenization of Heterogeneous Materials*, Wiley, 2016
6. Ł. Madej, Ł. Rauch, K. Perzyński and P. Cybulka, Digital Material Representation as an Efficient Tool for Strain Inhomogeneities Analysis at The Micro Scale Level, *Arch. Civ. Mech. Eng.*, 2011, **11**, p 661–679
7. K. Sobczyk and D.J. Kirkner, *Stochastic Modeling of Microstructures*, Birkhäuser Boston, Boston, 2001
8. L. Nastac and D.M. Stefanescu, Stochastic Modelling of Microstructure Formation in Solidification Processes, *Modell. Simul. Mater. Sci. Eng.*, 1997, **5**, p 391–420
9. A.B. Cruzeiro, Stochastic Approaches to Deterministic Fluid Dynamics: A Selective Review, *Water*, 2020, **12**, p 864. <https://doi.org/10.3390/w12030864>
10. P. Hahner, On the Foundations of Stochastic Dislocation Dynamics, *Appl. Phys. A*, 1996, **62**, p 473–481
11. D. Szeliga, N. Czyżewska, K. Klimczak, J. Kusiak, R. Kuziak, P. Morkisz, P. Oprocha et al., Formulation, Identification and Validation of a Stochastic Internal Variables Model Describing the Evolution of Metallic Materials Microstructure During Hot Forming, *Int. J. Mater. Form.*, 2022 <https://doi.org/10.1007/s12289-022-01701-8>
12. K. Klimczak, P. Oprocha, J. Kusiak, D. Szeliga, P. Morkisz, P. Przybyłowicz, N. Czyżewska and M. Pietrzyk, Inverse Problem in Stochastic Approach to Modelling of Microstructural Parameters in Metallic Materials During Processing, *Math. Probl. Eng.*, 2022 <https://doi.org/10.1155/2022/9690742>
13. D. Szeliga, N. Czyżewska, K. Klimczak, J. Kusiak, R. Kuziak, P. Morkisz, P. Oprocha, M. Pietrzyk, Ł. Poloczek and P. Przybyłowicz, Stochastic Model Describing Evolution of Microstructural Parameters During Hot Rolling of Steel Plates and Strips, *Arch. Mech. Civ. Eng.*, 2022, **22**, p 239. <https://doi.org/10.1007/s43452-022-00460-2>
14. Y. Kok, X.P. Tan, P. Wang, M.L.S. Nai, N.H. Loh, E. Liu and S.B. Tor, Anisotropy and Heterogeneity of Microstructure and Mechanical Properties in Metal Additive Manufacturing: A Critical Review, *Mater. Des.*, 2018, **139**, p 565–586
15. Y. Chang, M. Lin, U. Hangen, S. Richter, C. Haase and W. Bleck, Revealing the Relation Between Microstructural Heterogeneities and Local Mechanical Properties of Complex-Phase Steel by Correlative Electron Microscopy and Nanoindentation Characterisation, *Mater. Design*, 2021, **203**, p 109620
16. M.K. Singh, Application of Steel in Automotive Industry, *Int. J. Emerg. Technol. Adv. Eng.*, 2016, **6**, p 246–253

17. C.C. Tasan, M. Diehl, D. Yan, M. Bechtold, F. Roters, L. Schemmann, C. Zheng, N. Peranio, D. Ponge, M. Koyama, K. Tsuzaki and D. Raabe, An Overview of Dual-Phase Steels: Advances in Microstructure-Oriented Processing and Micromechanically Guided Design, *Annu. Rev. Mater. Res.*, 2015, **45**, p 391–431
18. Y. Chang, C. Haase, D. Szeliga, Ł Madej, U. Hangen, M. Pietrzyk and W. Bleck, Compositional Heterogeneity in Multiphase Steels: Characterization and Influence on Local Properties, *Mater. Sci. Eng., A*, 2021, **827**, p 142078
19. A. Karellova, C. Kremaszky, E. Werner, P. Tsipouridis, T. Hebesberger and A. Pichler, Hole Expansion of Dual-Phase and Complex-Phase AHS Steels—Effect of Edge Conditions, *Steel Res. Int.*, 2009, **80**, p 71–77
20. T. Henke, M. Bambach and G. Hirt, Quantification of Uncertainties in Grain Size Predictions of a Microstructure-Based Flow Stress Model and Application to Gear Wheel Forging, *CIRP Ann. Manuf. Technol.*, 2013, **62**(1), p 287–290. <https://doi.org/10.1016/j.cirp.2013.03.121>
21. D. Szeliga, Y. Chang, W. Bleck and M. Pietrzyk, Evaluation of Using Distribution Functions for Mean Field Modelling of Multiphase Steels, *Proc. Manuf.*, 2019, **27**, p 72–77
22. J.E. Warner, W. Aquino and M.D. Grigoriua, Stochastic Reduced Order Models for Inverse Problems Under Uncertainty, *Comput. Methods Appl. Mech. Eng.*, 2015, **285**, p 488–514
23. D. Szeliga, N. Jazdzewska, J. Forys, J. Kusiak, R. Nadolski, P. Oprocha, M. Pietrzyk, P. Potorski and P. Przybyłowicz, Sensitivity Analysis and Formulation of the Inverse Problem in the Stochastic Approach to Modelling of Phase Transformations in Steels, *Numerical Methods in Industrial Forming Processes: Numiform 2023*. J. Kusiak, Ł. Rauch, K. Regulski Ed., Springer, Cham, 2024, p 161–184. https://doi.org/10.1007/978-3-031-58006-2_13
24. Ł. Poloczek, R. Kuziak, J. Forys, D. Szeliga and M. Pietrzyk, Accounting for Random Character of Nucleation in Modelling of Phase Transformations in Steels, *Comput. Methods Mater. Sci.*, 2023, **23**(2), p 17–28
25. X. Liu, H. Li and M. Zhan, A Review on the Modeling and Simulations of Solid-State Diffusional Phase Transformations in Metals and Alloys, *Manuf. Rev.*, 2018 <https://doi.org/10.1051/mfreview/2018008>
26. A.F. Izmailov, A.S. Myerson and S. Arnold, A Statistical Understanding of Nucleation, *J. Cryst. Growth*, 1999, **196**, p 234–242
27. E. Clouet, Modeling of Nucleation Processes, in: ASM Handbook Vol. 22A, Fundamentals of Modeling for Metals Processing, Furrer D.U., Semiatin S.L., (Eds.), 2009, 203–219
28. S.E. Offerman, N.H. van Dijk, J. Sietsma, S. Grigull, E.M. Lauridsen, L. Margulies, H.F. Poulsen, M.T. Rekveldt and S. van der Zwaag, Grain nucleation and Growth During Phase Transformations, *Science*, 2002, **298**(5595), p 1003–1005. <https://doi.org/10.1126/science.1076681>
29. J.B. Leblond and J. Devaux, A New Kinetic Model for Anisothermal Metallurgical Transformations in Steel Including Effect of Austenite Grain Size, *Acta Metall.*, 1984, **32**(1984), p 137–146
30. H.K.D.H. Bhadeshia, *Bainite in Steels: Theory and Practice*, 3rd ed. Maney Publishing, Wakefield, 2015
31. Ł Madej, Y. Chang, D. Szeliga, W. Bleck and M. Pietrzyk, Criterion for Microcrack Resistance of Multi-Phase Steels Based on Property Gradient Maps, *CIRP Ann. Manuf. Technol.*, 2021, **70**(1), p 243–246
32. A. Saltelli, K. Chan and E.M. Scot, *Sensitivity Analysis*, Wiley, New York, 2000
33. D. Szeliga, Identification Problems in Metal Forming. A Comprehensive Study, Publisher AGH, no. 291, Kraków, 2013
34. Y. Rubner, C. Tomasi, L.J. Guibas, A metric for distributions with applications to image databases, in: IEEE International Conference on Computer Vision, Bombay, 1998, 59–66
35. M. Pietrzyk, Ł Madej, Ł Rauch and D. Szeliga, *Computational Materials Engineering: Achieving High Accuracy and Efficiency in Metals Processing Simulations*, Butterworth-Heinemann, Elsevier, 2015
36. J.C. Gelin and O. Ghouati, The Inverse Method for Determining Viscoplastic Properties of Aluminium Alloys, *J. Mater. Process. Technol.*, 1994, **34**, p 435–440
37. A. Gavras, E. Massoni and J.L. Chenot, An Inverse Analysis Using A Finite Element Model for Identification of Rheological Parameters, *J. Mater. Process. Technol.*, 1996, **60**, p 447–454
38. D. Szeliga, J. Gawąd and M. Pietrzyk, Inverse Analysis for Identification of Rheological and Friction Models in Metal Forming, *Comput. Methods Appl. Mech. Eng.*, 2006, **195**, p 6778–6798
39. D. Szeliga, N. Czyżewska, K. Klimczak, J. Kusiak, P. Morkisz, P. Oprocha, M. Pietrzyk and P. Przybyłowicz, Sensitivity Analysis, Identification and Validation of the Dislocation Density Based Model for Metallic Materials, *Metall. Res. Technol.*, 2021, **118**, p 317. <https://doi.org/10.1051/metal/2021037>
40. D. Bachniak, Ł Rauch, M. Pietrzyk and J. Kusiak, Selection of the Optimization Method for Identification of Phase Transformation Models for Steels, *Mater. Manuf. Processes*, 2017, **32**, p 1248–1259
41. D. Bachniak, Analiza Izogeometryczna Oraz Algorytmy Optymalizacji w Zastosowaniu do Projektowania Wieloetapowych Procesów Obróbki Ciepłej Stali w Czasie Kontrolowanego Chłodzenia, PhD thesis, AGH Kraków, 2021 (in Polish)

Publisher's Note Springer Nature remains neutral with regard to jurisdictional claims in published maps and institutional affiliations.